JOURNAL OF CATALYSIS **168,** 95–103 (1997)
ARTICLE NO. CA971632

# $BaFe_xAl_{(12-x)}O_{19}$ System for High-Temperature Catalytic Combustion: Physico-Chemical Characterization and Catalytic Activity

Gianpiero Groppi, Cinzia Cristiani, and Pio Forzatti

*Dipartimento di Chimica Industriale e Ingegneria Chimica "G. Natta" del Politecnico, Piazza Leonardo da Vinci 32, 20133 Milan, Italy*

Received October 24, 1996; revised January 14, 1997; accepted January 16, 1997

**Data on the physico-chemical characterization and on the catalytic activity in $CH_4$ combustion of $BaFe_{12}O_{19}$ and $BaFe_xAl_{(12-x)}O_{19}$ samples ($x = 1, 3, 6, 9$) are reported. $BaFe_{12}O_{19}$ shows good catalytic activity in $CH_4$ combustion, but does not possess the required thermal stability. It completely sinters upon calcination at temperatures higher than 1000°C and deactivates both on increasing the calcination temperature and upon treatment at 900°C under reaction conditions. The catalytic properties of this system completely degenerate upon calcination at 1300°C. Deactivation seems to be related both to sintering and to a $Fe^{3+} \rightarrow Fe^{2+}$ reduction involving limited metal amounts. Partial replacement of Fe ions with $Al^{3+}$ ions improves the thermal stability of the Fe-containing systems. Upon calcination at 1300°C $BaFe_6Al_6O_{19}$ retains a surface area of 5 $m^2/g$ and shows a good activity in $CH_4$ combustion.** © 1997 Academic Press

## 1. INTRODUCTION

Catalytic combustion is a promising method for the effective burning of lean fuel–air mixtures in gas turbine with ultra low emissions of $NO_x$, CO, and unburned hydrocarbons (1, 2). In view of the operating conditions of the combustor, catalytic materials able to resist at high temperature (1000–1300°C) are required. Moreover, the catalysts have to be active enough to light-off the fuel–air mixtures at low inlet temperatures ($T < 500$°C), fuel concentrations (2–3% of $CH_4$), and residence times (a few milliseconds) (1–3). Among the investigated systems high thermal stability has been reported for $BaMn_xAl_{(12-x)}O_{19}$ catalysts (4–6). These systems are monophasic with a Ba–$\beta$–$Al_2O_3$ structure in which $Al^{3+}$ ions are replaced by Mn. They exhibit a stable phase composition up to 1400°C and retain surface area of 12–17 $m^2/g$ upon calcination at 1300°C. This thermal stability has been related to the peculiar layered crystal structure consisting of the repetition of spinel blocks separated by conduction planes in which Ba ions are allocated. It has been observed that this structure is able to suppress crystal growth along the c-axis and consequently the sintering of the material up to 1400°C (4–7). The catalytic activity in $CH_4$ combustion enhances on increasing the Mn content in the structure up to $x = 2$. On further introduction of Mn in the structure ($x = 3$) the segregation of extraphases ($BaAl_2O_4$) and a drop of surface area (3, 4), but no enhancement of catalytic activity are observed (6, 8). A preliminary scale up of the laboratory data performed with a mathematical model of the catalytic combustor showed that Mn-containing systems are not active enough to meet the operating requirements of the combustor (9).

Fe ions have potential as alternative activity promoters in layered alumina structures. Among *M*-substituted hexaaluminates ($M$ = Mn, Fe, Co, Cr, Ni) with low *M*-content, Fe is reported as the second effective promoter, after Mn, of catalytic activity in $CH_4$ combustion (5, 10). Moreover a layered alumina structure has been reported to form over a wide range of Fe/Al ratio (11), including $BaFe_{12}O_{19}$, where Al ions are completely replaced by Fe ions. This material shows a magnetoplumbite-like structure that is closely related to $\beta$-$Al_2O_3$ (Fig. 1). Accordingly, Fe-substituted systems may potentially overcome the problem related to the limits on the *M*-content allocable in the structure observed in Mn-substituted catalyst.

In this paper we report on the results of characterization and catalytic activity tests for pure $BaFe_{12}O_{19}$ and for $BaFe_xAl_{(12-x)}O_{19}$ samples with $x = 1, 3, 6, 9$. The aim of the work is the comprehension of the influence of Fe ions content on the structural, morphological, and catalytic properties of the materials.

## 2. EXPERIMENTAL

### 2.1. Preparation

The $BaFe_xAl_{(12-x)}O_{19}$ samples ($x = 1, 3, 6, 9, 12$) have been prepared using the coprecipitation method (carbonates route) described elsewhere (6, 13).

Precursors of the final materials have been precipitated in aqueous medium by addition of $(NH_4)_2CO_3$ at constant $T$ (60°C) and pH (~7.5), starting from an acid solution of the constituent nitrates. After repeated washing and filtering to remove nitrates and $(NH_4)_2CO_3$ excess, the samples have been dried at 110°C. Chemical analysis (by



0021-9517/97 $25.00

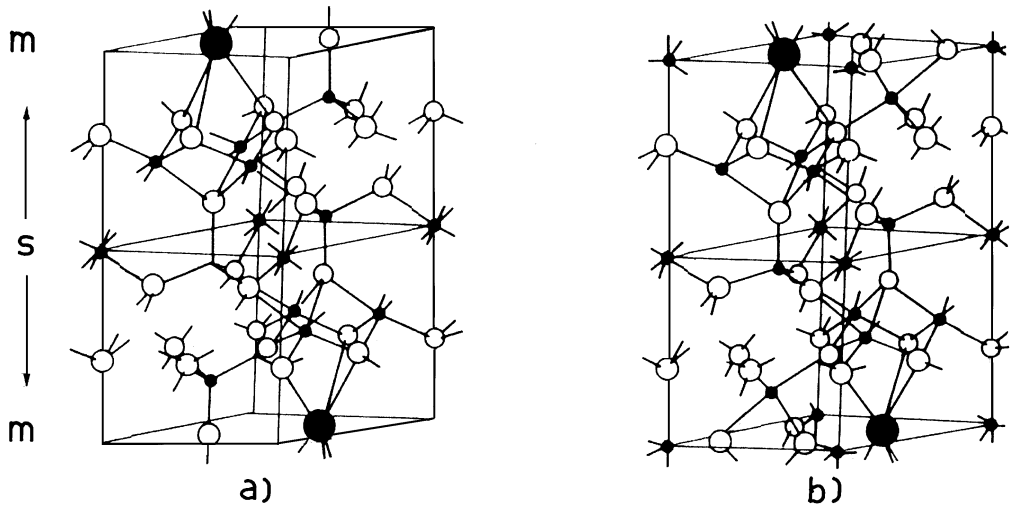


**FIG. 1.** Ideal semicells of (a) $\beta$-$Al_2O_3$ and (b) magnetoplumbite. ●, alkaline or alkali earth metal; ○, Oxygen ions; ●, Al or Fe ions; m, mirror plane; s, spinel block.

atomic adsorption) of mother liquors and washing waters evidenced that a quantitative precipitation has occurred. The dried samples were ground and then calcined by intermediate steps at 500, 700, 900, 1000, 1100, 1200, 1300, and 1400°C (heating rate, 60°C/h; holding at each step, 10 h; cooling rate, 100°C/h). Chemical analysis performed on the samples calcined at 1400°C confirms that the actual compositions of the samples well correspond to the nominal ones.

In the following the samples are identified by the constituent elements, the atomic ratios, and the calcination temperature: e.g., BaFe1Al11-900 indicates the sample with atomic ratios Ba/Fe/Al = 1/1/11 calcined at 900°C.

### 2.2. *Characterization*

XRD analyses have been performed by a Philips vertical goniometer PW1050-70, using a Ni-filtered Cu$K\alpha$ radiation ($\lambda$ = 1.54 Å). Crystallite dimensions have been evaluated by FWHM of the reflections using Sherrer equation (14). Lattice parameters have been calculated with a least-squares fitting routine, taking into account for systematic errors introduced by the goniometer.

DR–UV–Vis spectra have been recorded by a Jasco double-beam spectrophotometer equipped with an integrating sphere and a reference of $BaSO_4$ (spectral range, 250–850 nm; band width, 4 nm). In order to reduce the absorbance all the samples have been diluted with $BaSO_4$ according to the following procedure. The sample powders have been mixed with $BaSO_4$ and added with petroleum ether. The obtained slurry has been grounded in a mortar up to the complete evaporation of the ether.

Surface area measurements have been accomplished by nitrogen adsorption with the BET method using a Fison Sorptomatic 1900 Series Instrument.

Catalytic activity tests in $CH_4$ combustion have been carried out over powder catalyst in a quartz microreactor equipped with a sliding thermocouple for measurement of axial temperature profile. The reactor was filled with 0.5 $cm^3$ of catalysts powder ($d_p = 0.1$ mm) mixed with inert quartz powder $V_{cat.}/V_{in.} = 2$. Small particle size and dilution allowed for the suppression of external and internal heat and mass transfer limitation for $CH_4$ conversion below 20% as verified through a priori calculation (15). The tests have been performed under the following conditions: $P$, 1 atm; feed, 1% $CH_4$ in air; GHSV, 48.000 $h^{-1}$. Blank experiments have been obtained filling the reactor with the quartz powder only.

Reactants and products have been analyzed by on-line gas chromatography. After GC column separation, CO was converted to $CH_4$ before analysis with FID in order to ensure sensitivity at parts per million level. A detailed description of the analysis apparatus is reported elsewhere (6).

## 3. RESULTS

### 3.1. *BaFe12*

*Physico-chemical characterization.* The dried precursor BaFe12-110 is amorphous and upon calcination at 500°C only a poorly crystallized phase, likely $\gamma$-$Fe_2O_3$ [JCPDS 15-615] have been detected (Fig. 2a). Starting from 700°C the formation of crystalline $BaFe_{12}O_{19}$ [JCPDS 7-276], with magnetoplumbite-type (MP) structure, is observed (Fig. 2b). Upon further calcination up to 1300°C no changes in phase composition have been detected. Indeed BaFe12-1300 is monophasic (Fig. 2c), showing the reflections of a well-crystallized MP-type phase.

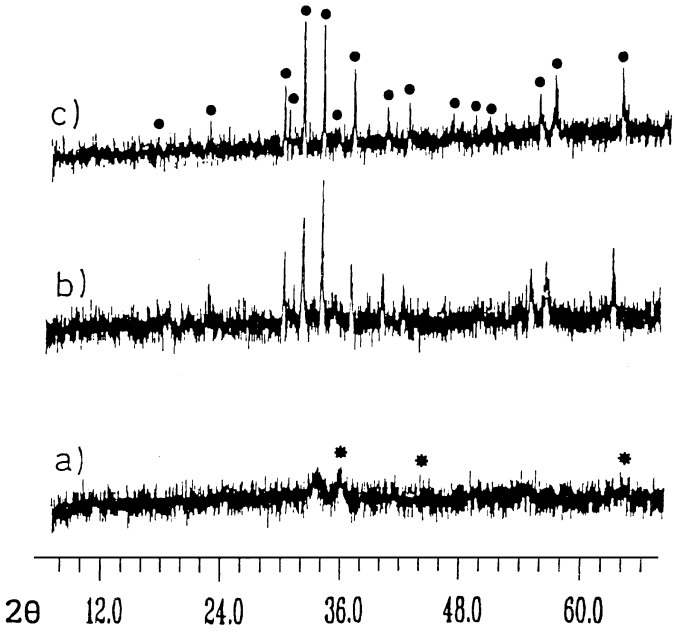


**FIG. 2.** XRD spectra of BaFe12 calcined at (a) 500, (b) 700, and (c) 1300°C. ●, $BaFe_{12}O_{19}$; ★, $\gamma$-$Fe_2O_3$.

Minor variations of the calculated MP lattice parameters are observed between 700 and 1300°C (BaFe12-700, $a_0 = b_0 = 5.91(1)$, $c_0 = 23.37(9)$ Å; BaFe12-1300, $a_0 = b_0 = 5.902(5)$, $c_0 = 23.26(3)$ Å). These values compare well with those reported in the literature ($a_0 = b_0 = 5.876$, $c_0 = 23.17$ Å [JCPDS 7-276]).

Despite the stable phase composition, the color varies from red–brown at 700°C to dark brown at 1000°C and finally to dark gray at 1300°C. It is reported in the literature that the interaction between the blue–violet $O^{2-} \rightarrow Fe^{3+}$ charge transfer (c.t.) and the red–orange $Fe^{2+} \rightarrow Fe^{3+}$ intervalence charge transfer (IVCT) band is responsible for the dark colors of some minerals even in presence of very small amounts of Fe ions with different oxidation states (16). Moreover very small variations of the relative amount of $Fe^{3+}$ and $Fe^{2+}$ species can result in marked color changes. This phenomenon can account for the variation of the dark colors of our samples and indicates that both $Fe^{3+}$ and $Fe^{2+}$ ions are present in the structure.

To further investigate this point, the DR–UV–Vis measurements have been performed on the calcined samples (Figs. 3a–3d). All the samples exhibit intense color which progressively darken on increasing the calcination temperature. This would result in saturation of the absorbance signal, so that the samples have been diluted with increasing amounts of $BaSO_4$. As a consequence in Fig. 3 the samples with the darkest colours show the lowest intensity of the DR absorption bands (e.g., compare Figs. 3a and 3d) and no quantitative considerations can be attempted.

The complex broad absorption centred at 450 nm in the spectrum of BaFe12-700 (Fig. 3a) can be attributed to *d–d* transitions of $Fe^{3+}$ in tetrahedral coordination (17, 18). Furthermore, the band observed at 730–740 nm can be associated with the $Fe^{2+}/Fe^{3+}$ IVCT band (19). On increasing the calcination temperature (Figs. 3b and 3c) the maximum at 450 nm smoothes and progressively shifts toward higher wavelengths (550 nm), while the IVCT band is always detected. In the spectrum of BaFe12-1300 (Fig. 3d) the maximum at 450 nm disappears and only a diffuse absorption in all the spectral range is observed in line with the dark grey color of the sample.

Studies on iron-containing minerals report that the transition bands of the tetrahedrally coordinated Fe(II) ions occur at wavelengths (689, 613, and 562 nm (20)) slightly higher than those of tetrahedrally coordinated Fe(III) (378, 458, 520, and 550 nm (20)). Accordingly the progressive shift of the maximum of the spectra, from 450 to 550 mn, can be attributed to a progressive thermal reduction of Fe(III) ions to give Fe(II). Also the diffuse absorption observed on the sample calcined at 1300°C is likely related to larger amount of $Fe^{2+}$ that results in a stronger overlapping of the bands associated with $Fe^{3+}$ and $Fe^{2+}$.

On the whole, the data indicate the co-presence in the final structure of both $Fe^{3+}$ and $Fe^{2+}$ species, with a progressive thermal $Fe^{3+} \rightarrow Fe^{2+}$ reduction due to the positive net rate of desorption of surface lattice oxygen at high temperature.

In order to investigate the extent of the reduction DTA-TG on BaFe12-700 and Mossbauer measurements on BaFe12 calcined at 700, 900, 1000, and 1300°C have

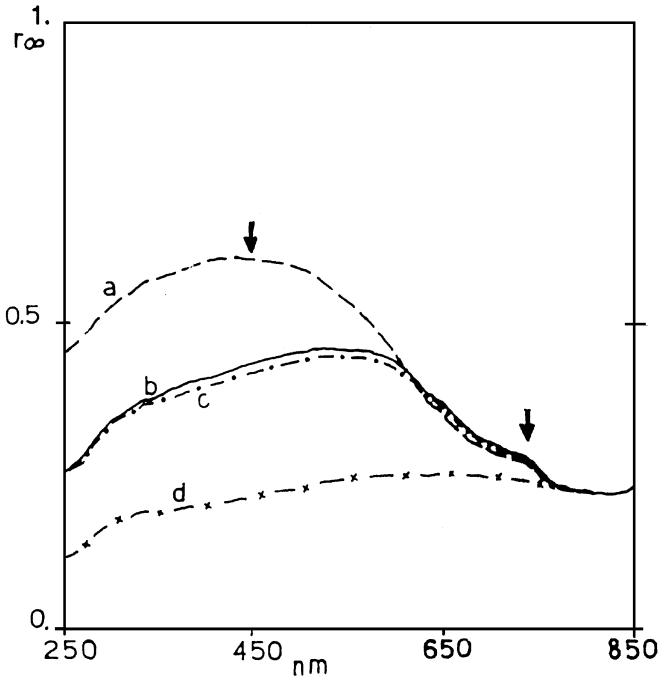


**FIG. 3.** UV–visible diffuse-reflectance spectra of BaFe12 calcined at (a) 700, (b) 900, (c) 1000, and (d) 1300°C.

been performed. No thermal effects and weight changes have been observed from room temperature to 1600°C in DTA-TG analysis. Besides no structural changes have been evidenced by Mossbauer spectra of the different samples. A very complex situation (five independent iron sites, each splitted in two components) which is consistent with the MP structure and with the presence of $Fe^{3+}$ ions only has been observed whereas no evidences of the presence of $Fe^{2+}$ or $Fe^0$ in the structure have been found.

DTA-TG and Mossbauer data show that only a small fraction of Fe ions, i.e., below the sensibility limits of these techniques, can participate in the reduction phenomenon. This is in line with the stability of the MP phase, up to 1300°C, which structure mainly allocates trivalent cations.

Surface area measurements have been performed on the samples calcined at different temperatures. The results show that (Fig. 4) the dried precursor BaFe12-110, exhibits high surface area (169 $m^2/g$) in line with its amorphous nature. Upon calcination at 700°C, the surface area value markedly decreases to 8 $m^2/g$ corresponding to the formation of the MP phase. The surface area keeps constant up to 1000°C, then it further decreases and above 1100°C it falls below the instrumental detection limit. A qualitatively increasing trend of the mean crystallite dimensions of the MP phase has been derived from FWHM that parallels the changes in surface area.

*Catalytic activity.* The data of $CH_4$ conversion vs reaction temperature obtained for BaFe12 calcined from 700°C up to 1300°C are reported in Fig. 5. The results of previous tests over a Mn-substituted hexaaluminate sample (BaMn2Al10-1300) (6) are also reported for sake of comparison.

Upon calcination at 700°C the Ba–hexaferrite catalyst shows an activity significantly higher than BaMn2Al10-1300. A 10% conversion of $CH_4$ is obtained at 425°C, about 100°C below the temperature required to obtain the same conversion with the Mn-containing sample. Despite

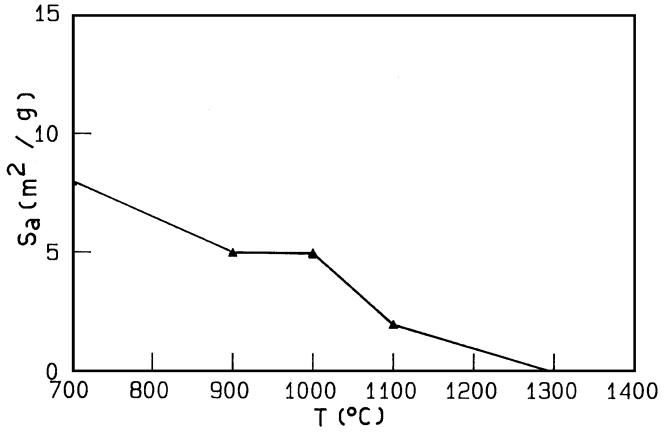


**FIG. 4.** Surface area of BaFe12 vs calcination temperature.

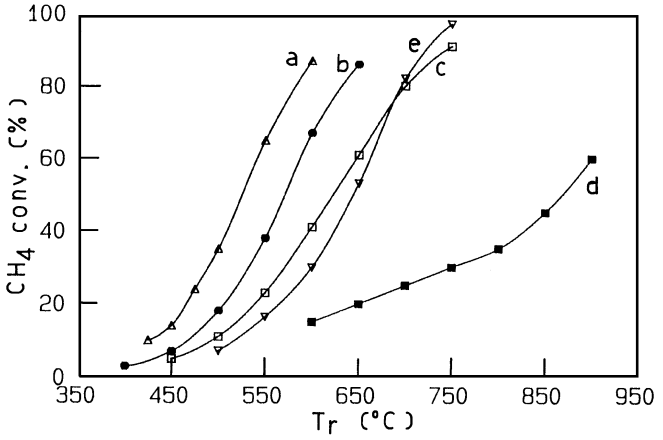


**FIG. 5.** $CH_4$ conversion vs reaction temperature over BaFe12 calcined from 700°C up to 1300°C. (a) BaFe12-700; (b) BaFe12-900; (c) BaFe12-1000; (d) BaFe12-1300; (e) BaMn2Al10-1300.

of the stable phase composition and surface area, the catalytic activity of BaFe12 progressively decreases on increasing the calcination temperature in the range 700–1000°C. At 1000°C the residual activity is comparable to that of BaMn2Al10-1300.

The catalytic activity of BaFe12 dramatically decreases upon calcination at 1300°C. This sample exhibits markedly lower conversion in the whole temperature range with an apparent activation energy of about 10 kcal/mol to be compared with the value of about 20 kcal/mol calculated for the samples calcined at lower temperature. Besides over BaFe12-1300 CO concentrations of 30–300 ppm have been detected in the products starting from 700°C, whereas no CO traces have been found with the other catalysts.

In order to study the stability of the catalysts under reaction conditions, catalytic activity tests have been repeated after aging the different BaFe12 samples at 900°C for 6 h under standard reaction atmosphere. For all the samples a marked decrease of the conversion at a given temperature has been obtained after the aging treatment: the observed deactivation roughly corresponds to the halving of the initial activity level. Once again BaFe12-1300 exhibits a peculiar behavior, its activity decreases of a factor 3–4 after only 1 h of treatment under reaction conditions.

Changes in the color of the samples have been observed after reaction at 900°C. The UV–Vis–DR spectra of these samples show that the complex absorption associated with $Fe^{3+}$ ions (≈450 nm) disappears after the aging treatment to give a diffuse absorption extended in the whole spectral range. It can be concluded that the aging at 900°C under reaction atmosphere, despite the relatively low temperature, causes a reduction phenomenon similar to that observed at high calcination temperature. This suggests that relatively small amounts of $CH_4$ (1%) can strongly promote reduction likely through a redox mechanism of the combustion reaction. Anyway, also in this case the aged samples maintain

the original MP crystal structure, thus indicating that only a small amount of Fe ions undergoes reduction.

### 3.2. *BaFexAl(12 − x) (x = 1, 6, 9)*

*Physico-chemical characterization.* In this section the results of characterization study on BaFe1Al11, BaFe6Al6, and BaFe9Al3 samples are presented.

Also a BaFe3Al9, which composition falls in the lack of miscibility range reported in the literature (11), has been prepared and characterized. A complex phase evolution has been observed and the simultaneous presence of both the Ba–$\beta$–$Al_2O_3$ and the MP phases has been detected up to 1400°C. Moreover, this sample shows the worst morphological and catalytic properties among the investigated systems. Accordingly, no data on this sample will be presented and discussed.

The dried precursors of BaFe1Al11 and BaFe6Al6 consist of a crystalline Al-containing phase ($(NH_4)_2Al_6(OH)_{14}(CO_3)_2 \cdot H_2O$) together with mixed Ba–Al hydroxide and/or hydroxicarbonate phases as already detected in the precursor of the Fe-free Ba−Al−O systems prepared according to the same procedure (6, 13). The dried precursor of $BaFe_9Al_3$ contains also microcrystalline Fe-oxides and crystalline $BaCO_3$ [Whiterite JCPDS 5-378].

In Table 1 the results of XRD of the $BaFe_xAl_{(12-x)}$ samples ($x = 1, 6, 9$) calcined above 1000°C are reported. The characterization data of BaFe12 and BaAl12 are also reported for the sake of comparison.

In all the Al-containing systems the formation of the layered alumina phase starts at considerably higher temperatures than that required by BaFe12. At low Fe contents (BaFe1Al11) the reflections of a Ba–$\beta$–$Al_2O_3$ phase appear in the XRD spectra only above calcination at 1100°C, the same temperature observed for the initial formation of the Ba–$\beta$–$Al_2O_3$ phase in Fe-free Ba–hexaaluminate samples (12). In the Fe-rich samples BaFe6Al6 and BaFe9Al3 the initial formation of the MP-type phase is observed already at 1000°C.

**TABLE 1**

**Thermal Evolution of the BaFe*x*Al(12 − *x*) Samples in the Temperature Range 1000–1400°C**

| Sample | Calcination temperature (°C) | | | |
|---|---|---|---|---|
| | 1000 | 1100 | 1300 | 1400 |
| BaFe12 | MP | MP | MP | MP |
| BaFe9Al3 | $BaAl_2O_4$, $\alpha$-$Fe_2O_3$ MP | $BaAl_2O_4$, $\alpha$-$Fe_2O_3$ MP | $\alpha$-$Fe_2O_3$ MP | $\alpha$-$Fe_2O_3$ tr. MP |
| BaFe6Al6 | $BaAl_2O_4$, MP | MP | MP | MP |
| BaFe1Al11 | $BaAl_2O_4$, $\theta$-$Al_2O_3$ tr., $\alpha$-$Al_2O_3$ | $BaAl_2O_4$, $\beta$-$Al_2O_3$ $\alpha$-$Al_2O_3$ | $\beta$-$Al_2O_3$ $\alpha$-$Al_2O_3$ | $\beta$-$Al_2O_3$ |
| BaAl12 | $BaAl_2O_4$ $\beta$-$Al_2O_3$ | $BaAl_2O_4$ $\beta$-$Al_2O_3$ | $\beta$-$Al_2O_3$ | $\beta$-$Al_2O_3$ |

*Note.* tr., traces.

**TABLE 2**

**Cell Parameters of BaFe*x*Al(12 − *x*) Calcined at 1400°C**

| Sample | Structure | Cell parameters (Å) | |
|---|---|---|---|
| | | $a_0 = b_0$ | $c_0$ |
| BaFe12 | MP | 5.902(1) | 23.27(4) |
| BaFe9Al3 | MP | 5.824(5) | 22.97(2) |
| BaFe6Al6 | MP | 5.734(5) | 22.68(2) |
| BaFe1Al11 | $\beta$-$Al_2O_3$ | 5.628(5) | 22.89(2) |
| BaAl12 | $\beta$-$Al_2O_3$ | 5.593(4) | 22.77(2) |

Complete formation of the final phase requires different temperatures depending on Fe/Al atomic ratio. However, upon calcination at 1400°C, monophasic systems have been obtained except for BaFe9Al3-1400 showing the presence of traces of $\alpha$-$Fe_2O_3$. According to the XRD analyses the nature of the final phase depends on the Fe/Al atomic ratio: BaFe9Al3 and BaFe6Al6 exhibit a MP-like structure similar to that of BaFe12, whereas BaFe1Al11 forms a Ba–$\beta$–$Al_2O_3$-like phase as in the case of Ba–hexaaluminate and Mn-substituted hexaaluminate systems (12, 6). The continuous enhancement of the cell parameters on increasing the Fe content (Table 2) confirm the presence of solid state solutions in the mixed Fe−Al samples. The results agree well with the phase diagram reported in the literature for the Ba–Fe–Al–O system with (Fe + Al)/Ba = 12 (21). According to this diagram MP-like phases form in the region of Fe-rich compositions and Ba–$\beta$–$Al_2O_3$ phases form in the region of Al-rich compositions. A lack of miscibility exists in the intermediate Fe/Al range (11).

BET measurements show that all the dried samples exhibit high surface areas (80–200 $m^2/g$) that progressively decrease on increasing the calcination temperature up to 1100°C. At this temperature all the samples show surface areas in the range 6–12 $m^2/g$, with the higher values corresponding to the higher Al content. The Fe/Al ratio also influences the sintering behavior at high temperature. Surface area does not change upon calcination at 1400°C in the case of BaFe1Al11 and BaFe6Al6 (∼5–7 $m^2/g$), while BaFe9Al3 progressively sinters and its surface area at 1300–1400°C is below the detection limit of the $N_2$ adsorption technique. It is worth noticing that the surface area of all the Fe-containing samples calcined at very high temperature are markedly lower than those measured for pure and Mn-substituted hexaaluminates (∼15 $m^2/g$ at 1300°C).

*Catalytic Activity*

Activity tests have been performed on the BaFe*x*Al(12 − *x*) samples calcined at 1300°C under the same experimental conditions used for BaFe12 samples.

Test results are reported in Fig. 6 in terms of $CH_4$ conversion as function of reaction temperature. For sake of comparison the conversion curves obtained over BaFe12-1300 and BaMn2Al10-1300 are also reported.

Upon calcination at 1300°C the activities of all the Fe-containing systems are lower than that of BaMn2Al10-1300. A different catalytic behavior is observed depending on the Fe/Al ratio. Similar conversion levels are obtained at 600°C but the apparent activation energy varies from 30 kcal/mol for BaFe6Al6-1300 to about 20 kcal/mol for BaFe1Al11-1300 and BaFe9Al3-1300 and, finally, to about 10 kcal/mol for BaFe12-1300. This results in the markedly different conversion observed at high temperature.

In the reaction products over the Fe-containing systems significant amounts of CO have been detected. In Fig. 7 are reported the CO concentration vs the reaction temperature measured over the BaFe$x$Al$(12-x)$-1300 samples together with the results of the blank experiments. Over BaFe1Al11-1300, BaFe6Al6-1300 and BaFe9Al3-1300 CO is a minor by-product corresponding to carbon selectivity always below 3%. It forms starting from 550–600°C and reaches a maximum at 750, 700, and 800°C, respectively. The maximum CO concentration markedly enhances on increasing the Fe content. On further increasing the temperature CO concentration decreases below the detection limit in the case of BaFe1Al11-1300 and BaFe6Al6-1300 and down to 40 ppm at 900°C in the case of BaFe9Al3-1300. The behavior of BaFe12-1300 markedly differs from those of the other Fe-containing samples showing CO formation only starting from 700°C with a gradual increase up to 350 ppm at 900°C corresponding to a carbon selectivity of 6%. Finally the blank experiments show formation of CO as the most abundant product (CO selectivity above 60%) starting from 800°C with a marked increase of concentration up to 900 ppm at 900°C. These data suggest that over

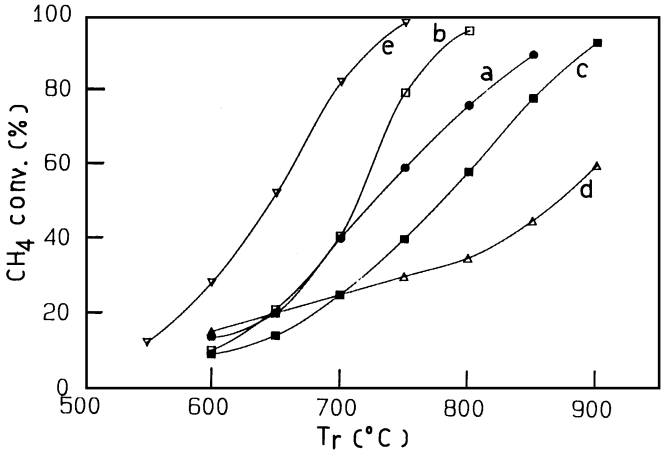


**FIG. 6.** $CH_4$ conversion vs reaction temperature over BaFe$x$Al$(12-x)$-1300 and $BaMn_2Al_{10}$-1300: (a) BaFe1Al11; (b) BaFe6Al6; (c) BaFe9Al3; (d) BaFe12; (e) BaMn2Al10.

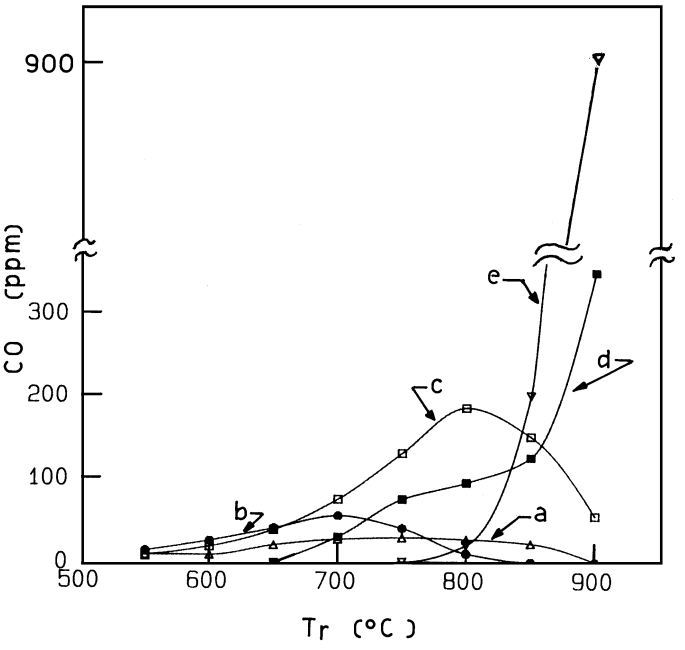


**FIG. 7.** CO concentration in the products of BaFe$x$Al$(12-x)$-1300. (a) BaFe1Al11; (b) BaFe6Al6; (c) BaFe9Al3; (d) BaFe12; (e) blank experiments.

BaFe1Al11-1300, and $BaFe_6Al_6$-1300, and BaFe9Al3-1300 CO forms as an oxidation product of the catalytic reaction with a concentration that vanishes, or at least markedly diminishes, before any significant contribution of the homogeneous reaction can occur. On the other hand, in the case of BaFe12-1300 the homogeneous reaction can play a significant role in CO formation in line with the very low activity of this sample.

The activity tests have been repeated after treatment at 900°C for 6 h under reaction conditions. In Table 3 the $CH_4$ conversion levels obtained at two reference temperatures before and after the treatment are reported. For BaFe1Al11-1300 and BaFe6Al6-1300 no significant

**TABLE 3**

**Effect of the Reaction Treatment on $CH_4$ Conversion over BaFe$x$Al$(12-x)$-1300**

| Sample | Reaction $T$ (°C) | % $CH_4$ conversion before treatment | % $CH_4$ conversion after treatment |
|---|---|---|---|
| BaFe1Al11 | 600 | 13.5 | 10 |
| | 650 | 22.9 | 20 |
| BaFe6Al6 | 600 | 10 | 8 |
| | 650 | 21 | 18 |
| BaFe9Al3 | 700 | 25 | 14 |
| | 750 | 40 | 25 |
| BaFe12 | 650 | 20 | 5 (1-h treatment) |
| | 700 | 25 | 9 (1-h treatment) |

variation are observed, being the differences of conversion in the range of the experimental error. On the other hand, for BaFe9-1300 and BaFe12-1300 a marked decrease in $CH_4$ conversion is observed after the treatment above.

## 4. DISCUSSION

### *4.1. $BaFe_{12}O_{19}$*

As reported elsewhere for Ba–Al–O systems (13) the preparation route here adopted results in the formation of a precursor with a good interspersion of the constituents: an amorphous material of high surface area (169 $m^2/g$) is obtained at 110°C. The formation of the crystalline MP phase occurs already at 700°C. It is worth noting that this temperature is 400–500°C lower than that required for the formation of the layered Ba–$\beta$–$Al_2O_3$ phase in the Ba-hexaaluminate systems (13). No further changes in the phase composition have been detected at higher temperatures and the only effect of the increasing temperature is a further crystallization of the MP-phase.

As observed for the Ba–Al–O system (13) also in the case of Ba–Fe–O system the formation of the final phase parallels a marked drop in surface area. Once the MP phase forms, the surface area is stable up to 1000°C, whereas a marked sintering is observed at higher temperature that results in the complete depletion of surface area upon calcination at 1300°C.

On the basis of experimental and literature results (7, 13), the following hypotheses can be drawn for the formation and sintering mechanism of $BaFe_{12}O_{19}$. Considering the structural isomorphism between the Al- and Fe-containing phases (12) the formation of the $BaFe_{12}O_{19}$–MP can occur via the same mechanism proposed for the Ba–$\beta$–$Al_2O_3$ (7, 13). This mechanism implies the diffusion of Ba ions within the oxygen close-packed planes of the defective spinel structure of $\gamma$-$Fe_2O_3$. Along this line the formation temperature of the final MP phase depends on the Ba mobility inside the original spinel structure. Accordingly the much lower threshold temperature required for the formation of the MP compared with that of Ba–$\beta$–$Al_2O_3$ can be attributed to an easier diffusion of Ba ions inside $\gamma$-$Fe_2O_3$. This greater ion mobility is in line with the behavior of the $\gamma \rightarrow \alpha$ phase transitions in Fe and Al oxides. These transitions imply oxygen mobility to allow for the rearrangement of the crystalline network and are reported to occur at about 300 and 700°C for $\gamma$-$Fe_2O_3$ (12) and at 900 and 1100°C for $\gamma$-$Al_2O_3$ in presence or not of alkali metals. This evidence provides a support for a lower threshold value for ion mobilisation in Fe–O spinel structure.

Once the MP crystallites formed they do not significantly sinter up to 1000°C. As in the case of Ba–$\beta$–$Al_2O_3$ (7, 12), one can hypothesize that the layered structure hampers the diffusion of Ba ions along the direction perpendicular to the conduction planes, hindering crystallite growth along the c axis and thus preventing the material from sintering. However, sintering inhibition is maintained only up to 1000°C, a temperature much lower than that of 1400°C observed in Ba–$\beta$–$Al_2O_3$. This behavior could be associated with the activation of the diffusion of Ba ions along the c direction of the layered MP phase starting from 1000°C in line with the greater mobility of Ba in the spinel-like blocks of iron than of aluminum oxides.

Although no changes in the phase composition have been observed above 700°C, progressive changing of the color of the samples has been detected on increasing the calcination temperature. According to the literature (22) this variation can be associated with the thermal reduction $Fe^{3+} \rightarrow Fe^{2+}$. This is in line with the results of UV–Vis–DR measurements. Indeed the progressive shift of the main absorption (450 nm) toward higher frequencies, and the presence of the $Fe^{3+} \rightarrow Fe^{2+}$ IVCT band, indicate that small amounts of $Fe^{2+}$ ions are present in the structure that increase with the calcination temperature. DTA-TG and Mossbauer analyses show that the fraction of $Fe^{2+}$ ions at all calcination temperatures fall below the detection limit of these techniques, thus indicating a limited extent of the $Fe^{3+} \rightarrow Fe^{2+}$ reduction. This is in line with the stability of the MP structure up to 1300°C.

At low calcination temperatures BaFe12 exhibits high catalytic activity in $CH_4$ combustion. BaFe12-700 provides a 10% conversion 100°C below $BaMn_2Al_{10}O_{19}$, i.e., the most active Mn-substituted Ba–hexaaluminate (6). However, the results of catalytic activity tests evidence that this system markedly deactivates both upon calcination at higher temperatures and upon treatment under reaction condition. Catalytic properties completely degenerate upon calcination at 1300°C; actually, BaFe12-1300 exhibits the lower $CH_4$ conversion, with significant amounts of CO detected in the products at high temperatures. It is evident that, despite of the close structural relation between MP and Ba–$\beta$–$Al_2O_3$, BaFe12–MP does not possess the stability required for high-temperature application. It is worth noting that neither phase composition nor surface area changes are observed in the temperature range 700–1000°C. Accordingly, within this temperature range, deactivation cannot be associated with sintering or phase evolution. On the other hand, sintering can play a role above 1000°C in view of the very low surface area of BaFe12-1300.

A mechanism has been proposed in the literature for $CH_4$ combustion over *M*-substituted layered alumina systems involving a redox cycle between (III) and (II) valences of the transition metal ion (4). In the MP structure of BaFe12 the oxidation state of the Fe ions is typically 3+; however, DR–UV–Vis evidence indicates that also a small amount of $Fe^{2+}$ ions is present. The simultaneous presence of divalent and trivalent Fe ions is consistent with the proposed redox mechanism. Along these lines the deactivation observed upon calcination and reaction treatment could be

associated with the $Fe^{3+} \rightarrow Fe^{2+}$ reduction described above. The data collected in this work do not provide direct indications on the nature of the reduction phenomenon. However, in view of its limited extent one can speculate that mainly Fe surface species are involved and this could also account for the dramatic effect observed on catalytic activity. Anyway, very small bulk contributions cannot be excluded.

### 4.2. $BaFe_xAl_{(12-x)}O_{19}$ ($x = 1, 6, 9$)

At 1400°C monophasic materials are obtained with the Ba–$\beta$–$Al_2O_3$ structure for BaFe1Al11 and with the MP one for Ba6Fe6Al6 and BaFe9Al3. This is in line with the literature (11, 21) showing that, upon calcination at high temperature, the BaFe$x$Al$(12-x)$ systems form monophasic materials in a wide composition range. Solid solutions are obtained due to similarity between $Al^{3+}$ and $Fe^{3+}$ ionic radii ($Al^{3+Td} = 0.39$Å vs $Fe^{3+Td} = 0.49$Å (23)). The partial substitution of Fe by Al ions in the structure inhibits the formation of the layered alumina phase and also affects the sintering behavior. As a general trend the sintering resistance of the final material enhances on increasing the Al loading. In fact, BaFe9Al3 markedly sinters upon calcination at 1300°C similarly to BaFe12, while BaFe6Al6 and BaFe1Al11 retain surface area of 5–7 $m^2$/g at high calcination temperature. Such values, however, are lower than those of $BaAl_{12}$ (15 $m^2$/g at 1400°C).

Also the catalytic behavior markedly depends on the Fe/Al ratio in the structure. As a whole BaFe6Al6-1300 exhibits the best catalytic properties among BaFe$x$Al$(12-x)$-1300: it shows the maximum $CH_4$ conversion, a good selectivity toward total oxidation, and a good stability under reaction atmosphere. Accordingly, this composition appears as the best compromise between the Fe content (combustion activity promoter) and the Al content (morphology and activity stabilizer) in the structure. BaFe1Al11 behaves quite similarly to BaFe6Al6 being only slightly less active despite of the wide difference on Fe content and the similar values of surface area. On the other hand, BaFe9Al3 exhibits much worse catalytic properties: it shows lower activity and markedly deactivates after treatment under reaction conditions at 900°C. This system behaves like BaFe12 showing that the Al content in its structure is not enough to provide a significant improvement of the thermal stability.

The stabilizing effect of Al ions on both morphological and catalytic properties can be somehow mutually related. As described above the sintering resistance of layered alumina structure is associated with the hampered diffusion of Ba (and oxygen) ions. This mechanism is strongly promoted by the Al ions as evidenced by the superior morphological properties of hexaaluminates and this is likely responsible for the stabilization of surface area through partial replacement of Fe ions with Al ones. The improved sintering resistance could also be responsible for the higher thermal stability of the catalytic properties. Moreover, the hindering of oxygen mobility due to the presence of Al ions can also affect the redox properties (e.g., rate and extent of $Fe^{3+} \rightarrow Fe^{2+}$ reduction) that in turn are related to the catalytic performances.

Finally it must be remarked that the catalytic activity of all the BaFe$x$Al$(12-x)$-1300 is lower than that of Mn-substituted hexaaluminate despite their higher content of transition metal ion. Accordingly Mn-substituted hexaaluminates remain the most suitable materials for high-temperature combustion.

## 5. CONCLUSIONS

In the present study the following main conclusions have been derived concerning catalytic, structural, and morphological properties of BaFe$x$Al$(12-x)$ systems:

(i) BaFe12 forms a monophasic material with MP-like layered-alumina structure similar to that of Mn-substituted hexaaluminates. The formation of the layered-alumina phase is completed at 700°C, i.e., 400–500°C below the temperature required by Mn-substituted hexaaluminates.

(ii) BaFe12 calcined at 700°C is very active in $CH_4$ combustion but it deactivates both upon increasing the calcination temperature and upon treatment at 900°C under reaction conditions. In particular, the catalytic properties of this system completely degenerate upon calcination at 1300°C. The observed deactivation phenomena could be associated both with sintering and with a partial $Fe^{3+} \rightarrow Fe^{2+}$ reduction.

(iii) The partial substitution of Fe ion within the layered alumina-type framework by massive quantity of Al significantly improves the thermal stability of Fe-containing systems. Upon calcination at 1300°C BaFe6Al6 show the best catalytic properties among BaFe$x$Al$(12-x)$. However, its activity is lower than that of Mn-substituted hexaaluminates.

## ACKNOWLEDGMENTS

This work has been supported by Ministero dell'Università e della Ricerca Scientifica e Tecnologica (MURST), Rome (Italy). Prof. Umberto Russo of Padova University and Prof. Francesco Berbenni of Pavia University are acknowledged for providing Mossbauer and DTA-TG measurements, respectively. The authors are in debt to Prof. Gilberto Artioli of Milano University for stimulating discussions and suggestions.

## REFERENCES

1. Pfefferle, L. D., and Pfefferle, W. C., *Catal. Rev. Sci. Eng.* **29**, 219 (1987).
2. Prasad, R., Kennedy, L. A., and Ruckenstein, E., *Comb. Sci. Technol.* **22**, 271 (1980).
3. Zwinkels, M. F. M., Jaras, S. G., and Menon, P. G., *Catal. Rev. Sci. Eng.* **35**, 319 (1993).

4. Machida, M., Eguchi, K., and Arai, H., *J. Catal.* **120**, 377 (1989).
5. Machida, M., Eguchi, K., and Arai, H., *J. Catal.* **123**, 477 (1990).
6. Groppi, G., Bellotto, M., Cristiani, C., Forzatti, P., and Villa, P. L., *Appl. Catal. A: Gen.* **104**, 101 (1993).
7. Groppi, G., Assandri, F., Bellotto, M., Cristiani, C., and Forzatti, P., *J. Solid State Chem.* **114**, 326 (1995).
8. Bellotto, M., Artioli, G., Cristiani, C., Forzatti, P., and Groppi, G., submitted for publication.
9. Groppi, G., Tronconi, E., and Forzatti, P., *Appl. Catal. A: Gen.* **138**, 117 (1996).
10. Groppi, G., Cristiani, C., and Forzatti, P., "Proceedings, XIV Simposio Iberoamericano de Catalisis," Vol. II, p. 773. Concepcion, Chile, September 12–16, 1994.
11. Batti, P., and Di Tella, F., *Annali Gazzetta Chim. Ital.* **57**, 74 (1967).
12. Wells, A. F., "Structural Inorganic Chemistry." Clarendon, Oxford, 1975.
13. Groppi, G., Bellotto, M., Cristiani, C., and Forzatti, P., *J. Mat. Sci.* **29**, 3441 (1994).
14. Klug, H. P., and Alexander, E., "X-Ray Diffraction Procedures." Wiley, New York, 1974.
15. Mears, D. E., *Ind. Eng. Chem. Process Des. Develop.* **10**, 541 (1971).
16. Faye, G. H., and Nickel, E. K., *Canad. Miner.* **10**, 617 (1970).
17. Manning, P. G., *Canad. Miner.* **10**, 677 (1970).
18. Moore, R. K., and White, W. B., *Canad. Miner.* **11**, 791 (1972).
19. Goldmann, D. S., and Rossman, G. R., *Amer. Miner.* **62**, 205 (1977).
20. Manning, G., *Canad. Miner.* **9**, 237 (1967).
21. Levin, E. M., Robbins, C. R., and McMurdie, H. F., "Phase Diagrams for Ceramists," M. K. Reser. Am. Ceram. Soc., 1985.
22. Cotton, F. A., and Wilkinson, G., "Advanced Inorganic Chemistry." Wiley, New York, 1972.
23. Huheey, J., "Inorganic Chemistry: Principles of Structure and Reactivity." Harper & Row, New York, 1972.